engineering proceedings

MDPI

Proceeding Paper

Studies on In Situ Alloy Formation Using Mild Steel–Inconel 625 Twin Filler Wire Gas Tungsten Arc Weld Deposition †

Denny Jacob John *, Koteswara Rao Sajja Rama, Lakshminarayanan K. Adhimoolam and Joshua Amalraj

Department of Mechanical Engineering, Sri Sivasubramaniya Nadar College of Engineering, Kalavakkam, Chennai 603110, Tamil Nadu, India; koteswararaosr@ssn.edu.in (K.R.S.R.); lakshminarayananak@ssn.edu.in (L.K.A.); joshuaa@ssn.edu.in (J.A.)

* Correspondence: dennyjacob94@gmail.com; Tel.: +91-8940768416

† Presented at the International Conference on Processing and Performance of Materials, Chennai, India, 2–3 March 2023.

Abstract: This work explored the possibility of producing a compositional functionally graded material (FGM) between mild steel and Inconel 625. An in-house fabricated, dual filler wire tungsten inert gas welding set up was used to deposit weld beads on a mild steel substrate. Filler wire feed rates were controlled independently and the combinations of filler material volumes, i.e., mild steel–Inconel 625 of (100:0), (75:25), (50:50), (25:75), and (0:100) were fed into the arc simultaneously and individual weld beads deposited. Preliminary studies revealed that defect free completely fused new alloys were formed and intermetallic phases rich in Nb observed. Compositional analysis showed that the content of each element changed from one alloy to the other gradually, smoothly indicating the feasibility of a mild steel–Inconel 625 functionally graded material.

Keywords: twin filler GTA welding; functionally graded materials; mild steel; Inconel 625; additive manufacturing

Citation: John, D.J.; Sajja Rama, K.R.; Adhimoolam, L.K.; Amalraj, J. Studies on In Situ Alloy Formation Using Mild Steel–Inconel 625 Twin Filler Wire Gas Tungsten Arc Weld Deposition. *Eng. Proc.* **2024**, *61*, 28. https://doi.org/10.3390/engproc2024061028

Academic Editors: K. Babu, Anirudh Venkatraman Krishnan, K. Jayakumar and M. Dhananchezian

Published: 1 February 2024

1. Introduction

Inspired by nature a new group of materials are being developed called functionally graded materials (FGM). FGMs were first developed in 1983 for the Japanese space shuttle project to reduce the thermal stress on the outer surface experienced by the shuttle upon re-entry into the earth's atmosphere [1–4]. These materials have received significance due to their graded structure, i.e., they exhibit one property (physical and chemical) on one side with a gradual change to another property on the other end and also perform effectively in extreme conditions without any significant loss of their performance [5,6]. In the field of aerospace, mineral processing, anti-ballistic applications, bio-materials, fire retardants, defense applications, nuclear reactors, chemical plants, etc., FGMs have become significant. FGMs are manufactured by different methods like layer remelting, chemical vapor deposition, powder metallurgy, welding, rapid prototyping, functionally graded coating, centrifugal methods, shape deposition manufacturing, laser engineered net shaping, electron beam selective manufacturing, directed energy deposition, and wire arc additive manufacturing (WAAM) [7,8]. A few examples of FGM are the SS321/IN 625 FGM fabricated by Mohan et al. for aerospace application by the WAAM technique [9] and Inconel 718/SS 316L FGM, successfully printed by Sang Hoon Kim et al. via DED, the chemical composition of the FGM being varied in steps of 10 wt% for the two materials across their build [10,11]. Kai-Chien Lo et al. created an FGM that enhances the corrosion resistance of coolant pipes at high temperature and under hydrostatic pressure of LBE (lead-bismuth eutectic) applications in nuclear power plants by the 3D laser printing technique [12]. This work focused on printing a mild steel (E7018)—Inconel 625 FGM on an in house fabricated dual filler GTAW-WAAM setup. The two filler wires were fed with controlled feed rates, thereby controlling the final composition of the weld.

2. Material and Methods

2.1. Equipment

The experimental WAAM setup is an in-house fabricated equipment containing a semi-automatic gas tungsten arc welding (GTAW) setup with a twin filler wire feeder and an argon shielding mechanism as shown in Figure 1. The filler wire of 1.2 mm diameter is fed into the torch by individual wire feeders. The wire feed is positioned at 45° so that the wires are fed directly into the core of the arc for the complete melting and deposition of the wires. With 160A of current, 140 mm/s of travel speed, and with a gas flow rate of 15 L/min, five beads of the proposed composition were achieved by controlling the wire feed of MS and IN 625 separately as 1840:0, 1720:900, 1540:1540, 900:1720, and 0:1840 MM/min for the proposed ratios, respectively. Here five individual beads of different composition as mentioned above were printed and subjected to mechanical and microstructural testing.

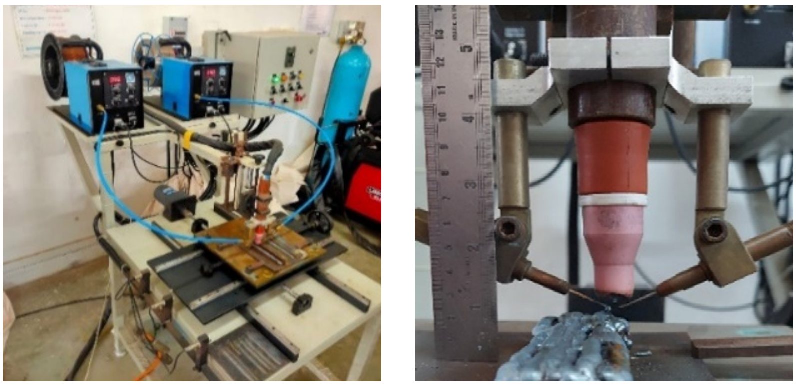

Figure 1. In-house fabricated twin Wire GTAW setup (**left**), the torch with wire feed setup (**right**).

2.2. Material Testing and Characterization

Cross-section samples of weld beads were cut by wire cut EDM from the deposited bead for the metallographic examination and hardness survey. Metallographic samples were mounted, polished as per the standards, and etched by Kalling's No. 2 reagent for 5 to 10 s. The macro and microstructure of the specimens were analyzed by optical microscopy and the elemental mapping was conducted using SEM equipped with an EDS analysis system. Micro-hardness profiles were measured at a load of 300 g and 0.1 mm distance between each point with a 10 s dwell time for each indentation using the Vickers hardness tester. Chemical analysis was performed by optical emission spectroscopy (OES).

3. Results and Discussion

The results of the experiments and the tests conducted over the cross-section of the weld bead are discussed below.

3.1. Microstructure

Macro-structure of the weld, 50%MS–50%IN (Figure 2a), shows a perfect semi-circular bead geometry and a perfect mixing of the two filler wires to form a new alloy. For each layer the layer-thickness of 4 mm (±1 mm) was achieved for all the five compositions. Figure 2b shows a complete ferrite–pearlite structure of mild steel with minimal dendritic structure. On the other hand, Figure 2f shows the micro-structure of Inconel which is completely a dendritic structure with primary and secondary arm structures. Figure 2c–e shows the transition of the micro-structure from a columnar to an equiaxed dendritic structure. Also, the increase in nickel content (austenite stabilizer) promoted the formation of the austenite phase. From Figure 2, it is seen that the addition of In 625 into the MS matrix has greatly influenced the formation of dendritic grains with austenite matrix.

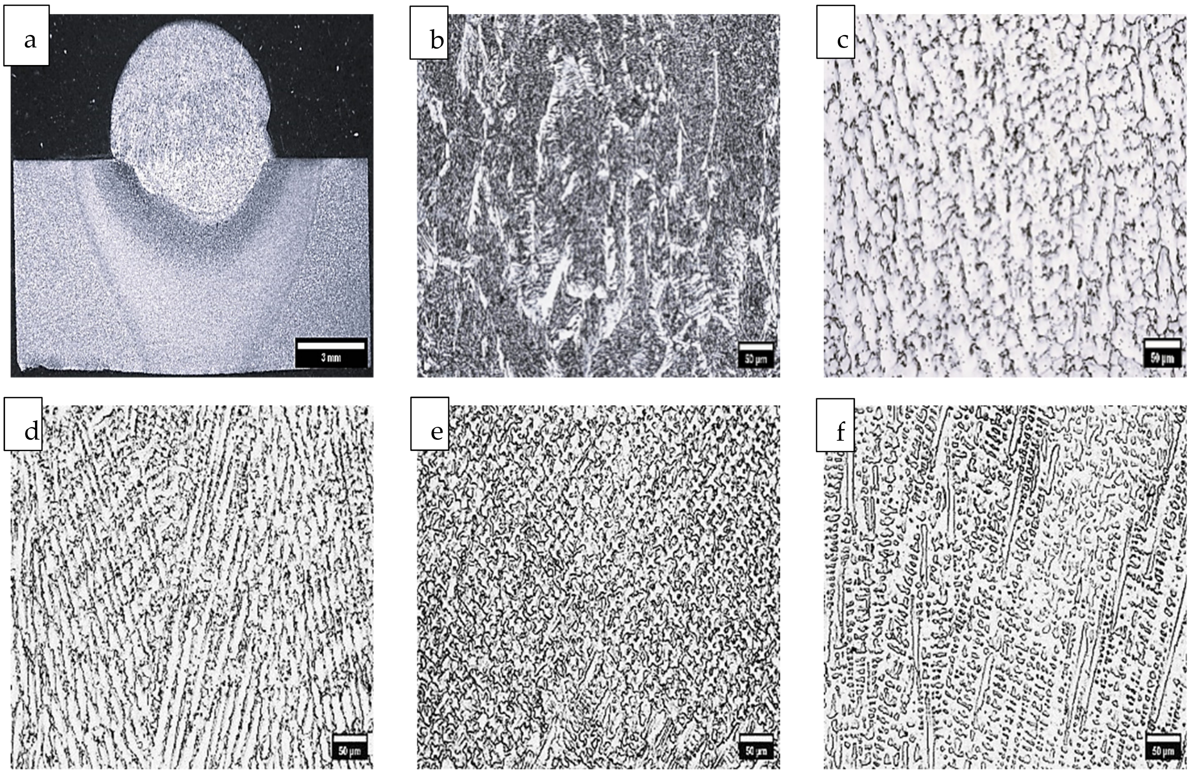

Figure 2. (**a**) CS macro structure of weld 50:50, (**b**) microstructure of 100:0, (**c**) microstructure of 75:25, (**d**) microstructure of 50:50, (**e**) microstructure of 25:75, (**f**) microstructure of 0:100.

In addition, from the SEM-EDS analysis, as shown in Figure 3, the point analysis carried out in the 50:50 sample shows that there is an increase in niobium content along the grain boundaries compared to the base matrix. From this, it can be concluded that the Nb forms some sort of precipitate and sits along the grain boundaries. There are two different phases observed: dark grey matrix (γ-matrix) and irregular bright white regions (laves phase). It is of note that the Nb and Mo content of the laves phase $(Ni,Fe,Cr)_2(Nb, Mo,Ti)$ has increased along the boundaries in comparison with the γ-matrix. Segregation of Nb and Mo in the interdendritic and grain boundaries has been reported [13,14].

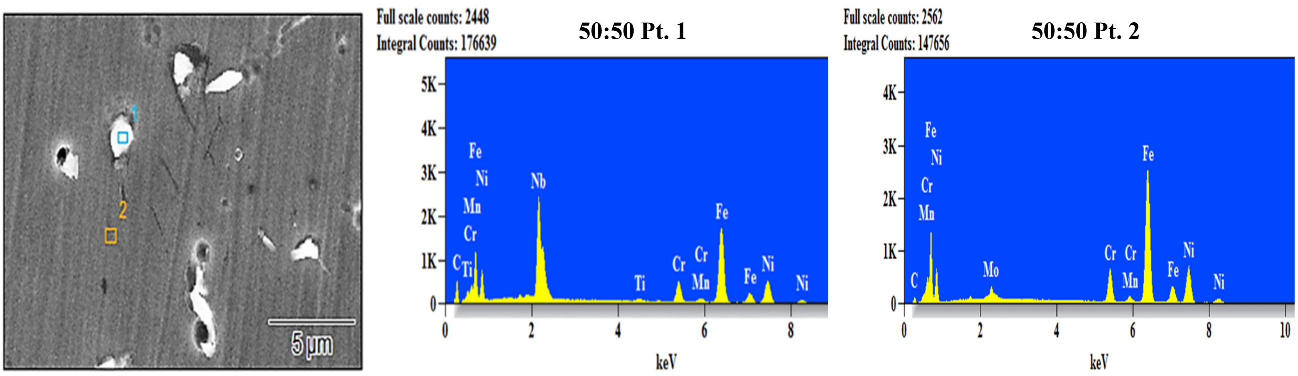

Figure 3. EDS point analysis report of the 50:50 sample.

3.2. Composition

The results of the OES analysis (average of two spots) are tabulated below. From Table 1, the chemical composition of each layer is found to be in-line with the desired wt% of FGM. The composition varied gradually from one end to the other end of the FGM.

Table 1. Chemical composition.

Sl.No.	Description	Weight%							
		Fe	C	Si	Mn	Cr	Mo	Nb	Ni
1	100:0	97.75	0.12	0.61	1.41	0.02	0.006	0	0.035
2	75:25	66.7	0.11	0.55	0.93	7.43	2.75	1.1	20.2
3	50:50	47.1	0.10	0.43	0.70	10.26	3.85	1.55	35.8
4	25:75	30.0	0.12	0.27	0.42	14.01	5.38	1.97	46.3
5	0:100	15.7	0.10	0.14	0.12	19.2	6.71	2.22	55.6

3.3. Hardness

The micro hardness survey was conducted at three different points vertically and 10 regions horizontally, and a total of 30 points were analyzed as shown in Figure 4. From the average hardness values, it is noted that the MS and IN 625 outer layers exhibited higher hardness values (225 and 205 VHN), respectively, while the core of the FG structure exhibited lower hardness values (142, 159, 184 VHN) attributed to the change in the microstructure and grain refinement as the IN 625 content increased. The sudden dip in the hardness of the 0.25 IN layer is due to the formation of an austenite phase by the addition of nickel.

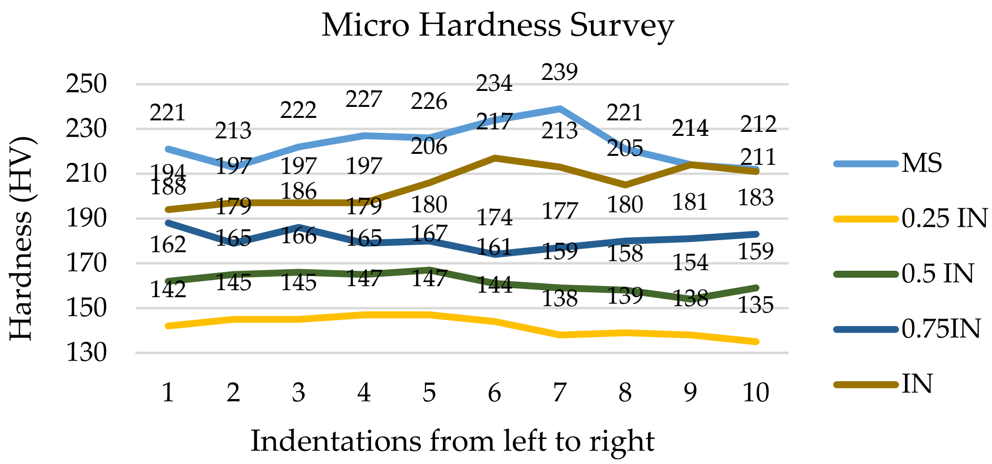

Figure 4. Hardness survey.

4. Conclusions

From the above results the following conclusions can be made:

- A twin filler gas tungsten arc weld setup was successfully used to produce MS–IN 625 FGM.
- The microstructure revealed a change from columnar to equiaxed dendritic with addition of Inconel 625 within the interlayers. Also, the addition of Ni to the MS matrix stabilized the austenite phase in the alloy.
- The EDS analysis revealed that Nb forms a precipitate along the dendritic grain boundaries while all other elements are distributed almost equally.
- The micro hardness survey showed hard outer layers (MS and IN 625) and a soft core with a gradual change of hardness in the interlayers with the addition of Inconel 625.

Author Contributions: D.J.J.—Methodology, formal analysis, investigation, writing—original draft preparation. K.R.S.R.—Conceptualization, validation, data curation, writing—review and editing, supervision. L.K.A.—validation, resources, project administration, J.A.—validation, visualization. All authors have read and agreed to the published version of the manuscript.

Funding: This research received no external funding.

Institutional Review Board Statement: Not applicable.

Informed Consent Statement: Not applicable.

Data Availability Statement: Data are provided in the manuscript.

Conflicts of Interest: The authors declare no conflict of interest.

References

1. Saleh, B.; Jiang, J.; Fathi, R.; Al-hababi, T.; Xu, Q.; Wang, L.; Song, D.; Ma, A. 30 Years of Functionally Graded Materials: An Overview of Manufacturing Methods, Applications and Future Challenges. *Compos. Part B Eng.* **2020**, *201*, 108376. [CrossRef]
2. Sasikumar, R.; Kannan, A.R.; Kumar, S.M.; Pramod, R.; Kumar, N.P.; Shanmugam, N.S.; Palguna, Y.; Sivankalai, S. Wire Arc Additive Manufacturing of Functionally Graded Material with SS 316L and IN625: Microstructural and Mechanical Perspectives. *CIRP J. Manuf. Sci. Technol.* **2022**, *38*, 230–242. [CrossRef]
3. Yu, X.; Xue, J.; Shen, Q.; Zheng, Z.; Ou, N.; Wu, W. Dual-Wire Plasma Arc Additively Manufactured SS 316L-Inconel 625 Functionally Graded Material: Microstructure Evolution and Mechanical Properties. *J. Mater. Eng. Perform.* **2023**, *32*, 1412–1422. [CrossRef]
4. Shen, C.; Pan, Z.; Cuiuri, D.; Roberts, J.; Li, H. Fabrication of Fe-FeAl Functionally Graded Material Using the Wire-Arc Additive Manufacturing Process. *Metall. Mater. Trans. B Process Metall. Mater. Process. Sci.* **2016**, *47*, 763–772. [CrossRef]
5. Boggarapu, V.; Gujjala, R.; Ojha, S.; Acharya, S.; Venkateswara babu, P.; Chowdary, S.; kumar Gara, D. State of the Art in Functionally Graded Materials. *Compos. Struct.* **2021**, *262*, 113596. [CrossRef]
6. El-Galy, I.M.; Saleh, B.I.; Ahmed, M.H. Functionally Graded Materials Classifications and Development Trends from Industrial Point of View. *SN Appl. Sci.* **2019**, *1*, 1378. [CrossRef]
7. Shen, C.; Liss, K.D.; Reid, M.; Pan, Z.; Hua, X.; Li, F.; Mou, G.; Huang, Y.; Dong, B.; Luo, D.; et al. Effect of the Post-Production Heat Treatment on Phase Evolution in the Fe_3Ni–FeNi Functionally Graded Material: An in-Situ Neutron Diffraction Study. *Intermetallics* **2021**, *129*, 107032. [CrossRef]
8. Wang, J.; Pan, Z.; Ma, Y.; Lu, Y.; Shen, C.; Cuiuri, D.; Li, H. Characterization of Wire Arc Additively Manufactured Titanium Aluminide Functionally Graded Material: Microstructure, Mechanical Properties and Oxidation Behaviour. *Mater. Sci. Eng. A* **2018**, *734*, 110–119. [CrossRef]
9. Mohan Kumar, S.; Rajesh Kannan, A.; Pravin Kumar, N.; Pramod, R.; Siva Shanmugam, N.; Vishnu, A.S.; Channabasavanna, S.G. Microstructural Features and Mechanical Integrity of Wire Arc Additive Manufactured SS321/Inconel 625 Functionally Gradient Material. *J. Mater. Eng. Perform.* **2021**, *30*, 5692–5703. [CrossRef]
10. Kim, S.H.; Lee, H.; Yeon, S.M.; Aranas, C.; Choi, K.; Yoon, J.; Yang, S.W.; Lee, H. Selective Compositional Range Exclusion via Directed Energy Deposition to Produce a Defect-Free Inconel 718/SS 316L Functionally Graded Material. *Addit. Manuf.* **2021**, *47*, 102288. [CrossRef]
11. Heydari, P.; Habibi, N. Parastoo Heydari. A Review on Functionally Graded-Thermal Barrier Coatings (FG-TBC) Fabrication Methods in Gas Turbines. *Am. J. Mech. Mater. Eng.* **2022**, *6*, 18–26.
12. Lo, K.C.; Lai, H.Y. Corrosion Enhancement for FGM Coolant Pipes Subjected to High-Temperature and Hydrostatic Pressure. *Coatings* **2022**, *12*, 666. [CrossRef]
13. Wang, J.F.; Sun, Q.J.; Wang, H.; Liu, J.P.; Feng, J.C. Effect of Location on Microstructure and Mechanical Properties of Additive Layer Manufactured Inconel 625 Using Gas Tungsten Arc Welding. *Mater. Sci. Eng. A* **2016**, *676*, 395–405. [CrossRef]
14. Cheepu, M.M.; Lee, C.; Cho, S.-M. Microstructural Characteristics of Wire Arc Additive Manufacturing with Inconel 625 by Super-TIG Welding. *Trans. Indian Inst. Met.* **2020**, *73*, 1475–1479. [CrossRef]